Water Air Soil Pollut (2026) 237:658
https://doi.org/10.1007/s11270-026-09344-0

Removal of Phenolic Compounds using Compost from Chicken Manure and Cardboard as Bulking Agent: Adsorption Tests and Cost Analysis

Khaled Al-Zawahreh · Remigio Paradelo

Received: 10 June 2025 / Accepted: 3 March 2026 / Published online: 10 March 2026

Abstract Recently, there has been increased interest in the use of composting to develop bioadsorbents for different pollutants. In this work, the removal of phenol, 2-nitrophenol, and 2,4-dinitrophenol from water is examined using compost derived from chicken manure (C/N ratio 6.3) and cardboard (C/N ratio 202.2) as a low-cost bulking agent. Characterization of the compost indicated its maturity, stability, and the presence of diverse surface functional groups. Toxicity Characteristic Leaching Procedure indicated that the bioavailability of toxic heavy metals including Cr, Pb, Cd, Zn, and Cu was negligible and below the regulated limits. Following a univariate experimental design, the effect of a number of operational factors on phenol adsorption by compost was assessed. The optimum operational factors for removing phenolic compounds are compost dosage 6.0 g L^{-1}, pH 2.0, contact time 80.0 min, and temperature 35.0 °C. The adsorption rate was adequately described using the pseudo-second order model, with relatively high estimated adsorption rates, 0.52–0.97 mg g^{-1} min^{-1}. Adsorption curves of phenols were adequately presented by the Langmuir model with maximum uptake capacity of 111.0 mg g^{-1} for phenol, 125.0 mg g^{-1} for 2-nitrophenol, and 134.0 mg g^{-1} for 2,4-dinitrophenol, comparable to other expensive adsorbents such as activated carbon, metal–organic frameworks or nano-adsorbents. The higher removal capacity of 2-nitrophenol and 2,4-dinitrophenol over phenol is attributed to higher solubility of phenol in water and the involvement of -NO_2 group in H-bonding with carboxylic group-rich-surface. The estimated production cost of compost is 0.04 USD per kg and 0.035 US Cent is needed to remove 1.0 g phenol from water.

Keywords Phenols · Compost · Chicken manure · Bulking agent · Cost analysis studies

Supplementary Information The online version contains supplementary material available at https://doi.org/10.1007/s11270-026-09344-0.

K. Al-Zawahreh
Department of Earth Sciences and Environment, Talal Faculty for Natural Resources and Environment, The Hashemite University, Prince El-Hassan Bin, P.O. Box 330127, Zarqa 13133, Jordan

R. Paradelo (✉)
CRETUS, Departamento de Edafoloxía e Química Agrícola, Facultade de Farmacia, Universidade de Santiago de Compostela, 15782 Santiago de Compostela, Spain
e-mail: remigio.paradelo.nunez@usc.es

1 Introduction

Contamination of water bodies, especially with organic pollutants, is a serious issue in the last few years. Organic pollutants have noxious consequences on humans due to their carcinogenicity and toxicity, and hence their occurrence in the water systems is unwanted (Ho, 2022; Ahmaruzzaman and Gadore, 2024). Among organic pollutants, phenol and its nitro-derivatives have harmful effects on humans even at low levels due to their carcinogenic, poisonous, and mutagenic nature (Ahmaruzzaman and Gadore 2024). Accordingly, they have been classified as priority pollutants by the US Environmental Protection Agency (US EPA, 2014). There are many industrial sources of phenolic compounds including coal coking petrochemical synthesis, and processing of natural materials like lignin, wood, and nutshells. The main anthropogenic sources of phenolic pollutants are from pharmaceutical, resin, plastic, and disinfectant industries (Ahmaruzzaman and Gadore, 2024). In addition, sustainable and natural sources of phenolic compounds resulted from agro-industrial waste like olive oil and rice bran production.

To prevent adverse taste and odor, the safe limit of phenol in drinking water was set at 0.001 mg L^{-1} (US EPA, 2014). Accordingly, developing effective methodologies for removing phenolic pollutants from wastewater is extremely important for environmental protection (Albadarin & Al-Zawahreh, 2025). Many cleaning technologies have been examined toward phenolic compounds, including biological degradation (Yang et al., 2016), ozonation (Honarmandrad et al., 2021), and adsorption (Albadarin & Al-Zawahreh, 2025; Bampi et al., 2024; Ho, 2022). Among cleaning technologies, adsorption utilizing natural and synthetic adsorbents, including activated carbon (Bampi et al., 2024; Ho, 2022), biomass (Sarker and Fakhruddin, 2017), zeolites (Khalid et al., 2004), clay composite (Adebayo & Areo, 2021), and metal organic frameworks (Liu et al., 2014), has been documented. Due to its simple design and convenient operating technique, efficient removal of a mixture of phenol and 4-nitrophenol by activated carbon has been reported (Bampi et al., 2024). Although activated carbon manifested excellent performance for removal of phenolic compounds, its high production cost along with tedious surface regeneration have encouraged researchers to develop other bioadsorbents for phenols (Sarker and Fakhruddin, 2017; Khalid et al., 2004; Albadarin & Al-Zawahreh, 2025). Recently, Albadarin and Al-Zawahreh have proposed a selection guide for the high-performance phenol adsorbents reported in the last five years (Albadarin & Al-Zawahreh, 2025). To be usable for cleaning wastewater, the adsorbent should be of high adsorption efficiency, removing multiple pollutants, and reusable for multiple adsorption–desorption cycles (Hossain et al., 2025). It is important to mention that adsorption technology was also found effective for removing micro and nano-size plastics from wastewater (Sajid et al., 2023).

Recently, researchers have become increasingly interested in using composted wastes as adsorbents for removing heavy metals (Liu et al., 2023; Ramisio et al., 2023) and organic pollutants (Al-Zawahreh et al., 2021, 2022, 2024a; Kyziol-Komosinska et al., 2024). The high adsorption capacity of compost for different pollutants is attributed to the existence of humic acid which are known for their high adsorption of different pollutants. As is known, composting is an aerobic biological decomposition of organic wastes, including municipal solid wastes, food scraps, and leaves, into a humic acid-rich product (Kyziol-Komosinska et al., 2024). This biological process, controlled by microorganisms, decreases landfill waste and lowers greenhouse emissions, reducing the need for high-cost chemical fertilizers (Liu et al., 2023; Ramisio et al., 2023). Chicken manure is an excellent candidate to produce stable and mature compost, as it is an N-rich feedstock with a low C/N ratio of 5–15 (Rynk et al., 2021), and it benefits from the addition of bulking agents, which enhances substrate properties such as air and water content, density, and C/N ratio, positively affecting the decomposition rate (Ahn et al., 2007; Yun et al., 2025). Basically, bulking agents are the backbone of the composting process, as they improve aeration, improve structure, and balance moisture (Mussa et al., 2025; Yun et al., 2025). Bulking agents, including straw, sawdust, and wood chips, can absorb excess moisture and create air spaces, which are necessary for the activity of microorganisms to break down the organic feedstock (Mussa et al., 2025; Yun et al., 2025). Moreover, bulking agents can balance out the C/N ratio, which is important for effective composting. In this regard, forestry and agricultural waste are often used as bulking agents, including cotton waste (Paredes et al., 2000), hay (Barrington et al., 2002), pine shavings, chestnut burr and leaves (Barrington et al., 2002; Wang et al., 2004), or cereal straw (Barrington et al., 2002). These present high C content, high C/N ratio, and low moisture that can compensate for the opposite values of the animal manures (Abolhassani et al., 2023; Bernal et al., 2009; Rynk et al., 2021). Other than composting, conversion of organic wastes into biochar has received high attention as indicated in the recent literature (Ihsanullah et al., 2022).

In continuation of our previous research on utilizing compost as bioadsorbent (Al-Zawahreh et al., 2021, 2022, 2024a), here we investigated the removal of phenol, 2-nitrophenol, and 2,4-dinitrophenol from water using compost derived from chicken manure and cardboard as a low-cost bulking agent. Up to authors` knowledge, using cardboard as a bulking agent in composting chicken manure was not reported before. For safe use of the bioadsorbent, the maturity, stability, and bioavailability of toxic metals were monitored during composting using various physiochemical methods. Factors affecting adsorption of phenolic compounds, including compost dosage, solution pH, contact time, salinity, and temperature, were optimized before running kinetic and equilibrium tests, and the mechanisms of interaction with compost were also addressed. The performance of compost as an adsorbent is compared with other nonconventional and commercial adsorbents, considering the variations in their production costs.

2 Materials and Methods

2.1 Composting Process

Chicken manure, the source of nitrogen, was collected from a chicken farm within the city of Amman (Jordan). Cardboard, the source of carbon and a bulking agent was collected from local supermarkets in Al-Mafraq city (Jordan). The cardboard was cut into small pieces measuring 1.0–1.5 cm. The main composition of the feedstocks is provided in Table 1. Composting was carried out for 10 weeks in a 250-L silo composter. For chicken manure, a level of two parts to one part cardboard (the bulking agent) is often recommended because of the high nitrogen content in the manure. To provide aeration and to dissipate the heat generated during the thermophilic phase, feedstocks in the composter were turned over weekly till the end of the process. Moisture content was maintained at 50–60% by manual spraying tap water while turning the contents to provide satisfactory aeration for microorganisms. A 5.0–10.0 g sample was gathered from the composter over different parts, depths (0–50 and 50–80 cm) and periods to monitor composting process and the quality indicators of the final product including moisture, ash, total organic carbon, total nitrogen content, ammonium/nitrate ratio, and C/N ratio.

Table 1 Physicochemical characteristics of the feedstock

Parameter	Chicken manure (N-source)	Cardboard/ Bulking agent (C-source)
pH	7.3	7.4
Moisture (%)	74.6	11.2
Total organic carbon (%)	30.2	46.5
Total N (%)	4.81	0.23
Total P (%)	3.51	0.11
Total K (%)	2.11	1.01
C/N ratio	6.3	202.2

2.2 Compost Characterization

Samples from different stages of composting (from week 1 to week 10) were collected weekly, dried and crushed in preparation for chemical analysis. For each sample, moisture, ash, total organic carbon, total nitrogen content, ammonium/nitrate ratio, C/N ratio, and temperature were analyzed to evaluate the quality of the composted material as outlined in the literature (Biyada et al., 2020). Surface functional groups were detected by running FTIR analysis; spectra were taken over the range 400 to 4000 cm^{-1} and with a 2.0 cm^{-1} resolution. The samples were extracted with 0.5 M NaOH and the absorbance values at 280 and 660 nm were used to estimate the ratio A_{280}/A_{660} in order to evaluate the degree of humification in the final product (Biyada et al., 2020). Finally, the bioavailability of toxic metals, including Pb, Cd, Cr, Cu, and Zn, was performed using the Toxicity Characteristic Leaching Procedure (TCLP), where compost is contacted with a simulated municipal landfill leachate and analyzed by inductively coupled plasma-atomic emission spectroscopy (ICP-AES).

2.3 Phenols Removal Experiment

2.3.1 Chemicals, Solutions and Instruments

With a purity of 99.9%, phenol (Ph), 2-nitrophenol (2-NPh), and 2,4-dinitrophenol (2,4-DNPh) were purchased from SIGMA-ALDRICH® (USA).

Table 2 Structural formulae with some important physicochemical parameters of the examined phenols[a]

IUPAC name	Structural formula	Acidity pK_a	Solubility in water, g/L (20 ºC)	Partition coefficient Log P	λ_{max} (nm)
Phenol (Ph)	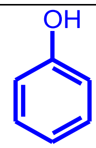	9.89	93.0	1.48	270.0
2-Nitrophenol (2-NPh)	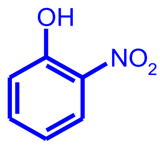	7.17	2.0	1.79	270.0
2,4-Dinitrophenol (2,4-DNPh)	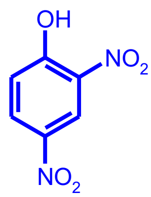	4.11	5.6	1.89	352.0

[a]Physicochemical parameters were collected from NIH (2025) and Dąbrowski et al. (2005)

Double-distilled water was used for solution preparation and throughout the experimental work. As summarised in Table 2 (NIH, 2025; Dabrowski et al., 2005), the tested phenols have variable acidity and 2,4-dinitrophenol was the most acidic with pK_a 4.11. Moreover, phenol exhibited a high solubility in water of 93.0 g L^{-1}. 2,4-dinitrophenol have the most hydrophobicity with a Log P of 1.89. For each adsorbate, a stock solution (1000 mg L^{-1}) was prepared by dissolving 1.0 ($\pm$0.0001) gram in 10.0 mL distilled water. All working solutions were prepared from the stock solutions after appropriate dilution. A Thermo Scientific UV–Vis spectrometer was used to perform spectral analysis of phenolic compounds in the 200–450 nm range (Thermo Scientific, USA). High-purity KCl crystals and 0.1 M HCl and NaOH standard solutions were purchased from Sigma–Aldrich®. Agitation of solutions was carried out using a mechanical thermostated shaker (GFL, Germany). Whatman filter paper no. 5 was used to isolate compost from the solution.

2.3.2 *Factors Affecting Phenolics Retention by Compost*

Univariate Optimization An optimized univariate design was adopted to study the effect of operational factors on phenols uptake as shown in Table 3, with four levels assessed for each factor. A twenty-experiment adsorption test was carried out to optimize the examined factors for phenol uptake by compost. In all tests, the initial level for each phenol was maintained at 100 mg L^{-1}. Typically, a fixed amount of dried compost (particle size 300–500 µm) was contacted with 50 mL of adsorbate solution at a certain concentration in a 250-mL volumetric flask. The flask was tightly closed and agitated using a thermostated shaker at 150 rpm and at a preselected temperature. After equilibrium, the flask was removed, and particles of compost were isolated using centrifugation at 5000 rpm. The remaining level of each phenol was measured using spectrophotometry. The absorbance values at 270, 338, and 352 nm were used to estimate the remaining concentrations of Ph, 2-NPh, and 2,4-DNPh from a pre-constructed calibration curve for each solute.

2.3.3 *Kinetic and Equilibrium Studies*

The rate of phenol uptake by compost was studied as follows: 6.0 g of dried compost were added to 1000 mL of 100 mg L^{-1} phenol solution at pH 2.0, under stirring. Aliquots (1.0–1.5 mL) were withdrawn from the solution over the following time intervals: 0, 10, 20, 30, 40, 60, 80, and 100 min, filtered, and the

Table 3 Univariate-based experimental design for studying the effect of operational factors on phenols uptake by compost using batch process[a]

Factor Effect	Factors			
	Dosage (g/L)	pH	Contact time (min)	Temperature (°C)
Dose effect	2.0, 4.0, **6.0**, 8.0[b]	4.0	80	25
pH effect	6.0	**2.0**, 4.0, 6.0, 8.0	80	25
Ionic strength effect	6.0	4.0	80	25
Contact time effect	6.0	4.0	40, 60, **80,** 100	25
Temperature effect	6.0	4.0	80	20, 25, 30, **35**

[a]In all tests, phenols level was 100 mg/L and agitation rate 150 rpm

[b]The highlighted data indicate the optimum uptake of phenols by compost

concentration of the remaining adsorbate was measured as described previously. This was repeated for 2-NPh and 2,4-DNPh.

For equilibrium studies, a series of phenol solutions was prepared in 150 mL flasks, covering the range from 0 to 1000 mg L^{-1}. For each solution, pH was adjusted at 2.0 after adding compost at a 6.0 g L^{-1} dose (0.300 g/50 mL). The flasks were placed in the shaker and agitated for 80 min at 25ºC. The mixtures were then filtered to isolate compost in preparation for spectroscopic quantification as outlined earlier. The test was repeated for 2-NPh and 2,4-DNPh.

2.4 Modeling of Adsorption Data

Mass balance equations, kinetic models, isotherms, and error function are provided in Table SM1 in Supplementary Material. Reaction-based and diffusion-based models were applied to model kinetics of phenols uptake from solution. All adsorption parameters were estimated by non-linear regression analysis using Origin Pro2016® software. Kinetic curves and isotherms were generated by Origin Pro2016® software. The average relative error (ARE) was used to evaluate the closeness between experimental and model-predicted results as outlined in Supplementary Material.

3 Results and Discussion

3.1 Compost Properties and Effect of Bulking Agent

Due to the substantial effects of chicken manure on the ecosystem, it could be transformed into eco-friendly byproducts (Abolhassani et al., 2023; Bernal et al., 2009). As indicated in Table 1, chicken manure was rich with N with a C/N of 6.3 and high moisture content, 74.6%. The high moisture content makes the manure dense and may not be suitable for aerobic composting. On the other hand, the bulking agent is suitable to balance out carbon content with C/N 202.2, as shown in Table 1. The changes in temperature, moisture, ash and ammonium/nitrate ratio reflect the progress of composting process. As shown in Table 4, temperature was notably increased during the first five weeks (45–59 °C) and gradually reduced to reach 24.2 °C in the last week. The high increase in the temperature was attributed to the intense microbial activity during the thermophilic stage of composting (Vergnoux et al., 2009). In conjunction with the rise in temperature, there was a clear decrease in the moisture content, as it reduced from 66.4 to 18.3% at the end of composting process. On the other side, the intense biological degradation of organic materials led to a decrease in acidity at the end of the process as shown in Table 4. The values of the C/N ratio during the first composting weeks were very high, 48–51, and its notable reduction during composting is evidence of the breakdown of organic materials by microorganisms, which resulted in the release of CO_2 simultaneously with an increase in N content (Biyada et al., 2019). The final compost is stable and mature with C/N ratio 20 and this supports that using cardboard as a C-rich source and bulking agent was helpful for accelerating the rate of biodegradation. The ammonium/nitrate ratio reflects the success of the composting process and the maturity of the final product; it is often recommended to be under 1.0 (Biyada et al., 2019). As shown in Table 4, the ammonium/nitrate

Table 4 Measured physicochemical parameters during composting

Time	Temp (°C)	Moisture (%)	Ash (%)	pH	TOC (%)	TN (%)	C/N	NH_4^+/NO_3^-	A_{280}/A_{660}
Initial	22.3	66.4	33.2	7.22	57.3	1.13	51	22.7	54.2
Week 1	45.4	43.2	39.1	7.11	51.3	1.12	46	21.3	51.3
Week 2	49.1	39.4	41.4	7.05	48.3	1.01	48	19.4	49.3
Week 3	51.3	31.2	42.4	7.00	41.3	0.93	44	18.1	44.2
Week 4	55.1	29.4	44.2	7.01	37.2	0.91	41	17.3	41.5
Week 5	59.4	28.1	44.1	6.77	31.2	0.87	36	15.2	38.4
Week 6	47.5	27.1	47.3	6.45	29.1	0.81	36	10.4	33.2
Week 7	38.2	21.4	49.3	6.17	19.3	0.77	25	8.3	29.1
Week 8	31.6	20.4	50.2	6.17	17.8	0.71	25	4.5	22.3
Week 9	29.0	19.1	51.3	6.22	16.1	0.68	24	1.0	21.5
Week 10	24.2	18.3	52.4	6.19	12.8	0.63	20	0.6	19.4

ratio decreased from 22.7 down to 0.6, also indicating that the compost derived from chicken manure and cardboard is mature.

UV–Vis spectroscopy can provide further evidence of organic matter transformations during composting process. The absorbance measured at 280 nm (A_{280nm}) evidences the presence non-humified material like lignin and quinone in the initial feedstock (El Hajjouji et al., 2007), while the absorbance at 660 nm (A_{660nm}) indicates the humification of organic material and presence of condensed aromatic rings (Albrecht et al., 2011). Thus, the absorbance ratio A_{280nm}/A_{660nm} measures the ratio between unhumified and humified components in compost (Ding et al., 2020). Hence, the reduction of A_{280nm}/A_{660nm} ratio with composting time evidences the higher rate of aromatic condensation and stabilization of the final product. As shown in Table 4, the ratio A_{280nm}/A_{660nm} was highly reduced after 50 days of composting due to the high contents of carboxylic and phenolic compounds of humic materials in the final product. During the last two weeks of composting, the ratio A_{280nm}/A_{660nm} was stabilized at 19–21, which indicates that the prepared compost was stabilized and reached the maturity state. Based on UV–Vis analysis, compost reached maturity and with a high fraction of humic acid, what is positive for use as bioadsorbent.

FTIR spectroscopy can also be applied to characterize functional groups after humification of organic matter (El Ouaqoudi et al., 2015; Paradelo et al., 2020). The FTIR spectrum of the final compost is presented in Fig. 1, with the main IR peaks at 3380, 3000, 2900, 2160, 2030, 2000, 1600, 1420 and 1070 cm^{-1}. This evidenced the presence of plenty of chemical bodies including aromatic, aliphatic and polysaccharide in the compost (Ding et al., 2020). The broad band at 3380 cm^{-1} is attributed to the stretching vibration of –OH group and hydroxyl group of COOH. The bands at 3000 and 2900 cm^{-1} are attributed to stretching vibrations of aliphatic C-H bond, signifying the skeleton of many biomolecules. The bands over the range 2200–500 cm^{-1} can evidence the presence of different functional groups that developed during composting process. The strong IR peak at 1600 cm^{-1} is due to the overlapping of aromatic C = C vibrations, alkene C = C vibrations, O–H in H_2O, and C = O vibrations in carboxylates and amides functional groups (Smidt & Meissl, 2006). The short band at 1530 cm^{-1} is attributed to vibrations of aromatic C = C, aromatic skeleton of lignin and vibrations of C≡N containing compounds (Ahmad et al., 2017). The same band can also indicate the presence of amide II in the sample. The sharp band at 1420 cm^{-1} can evidence the presence of carbonate species, alkyl groups and/or O–H in phenolic groups. The strong band at 1000 cm^{-1} is assigned to C–OH, C–O, C–O–C stretching of polysaccharide-like materials in the complex with humic acids (Ahmad et al., 2017). Moreover, the band at 1000 cm^{-1} would be attributed to the S–O stretching vibration (Smidt & Meissl, 2006). The bands at 825 and 680 cm^{-1} are both assigned to the aromatic ring and –C = S = C–, respectively, or to NH_2 out-of-plane vibrations of primary amine groups (Smidt & Meissl, 2006). Important changes

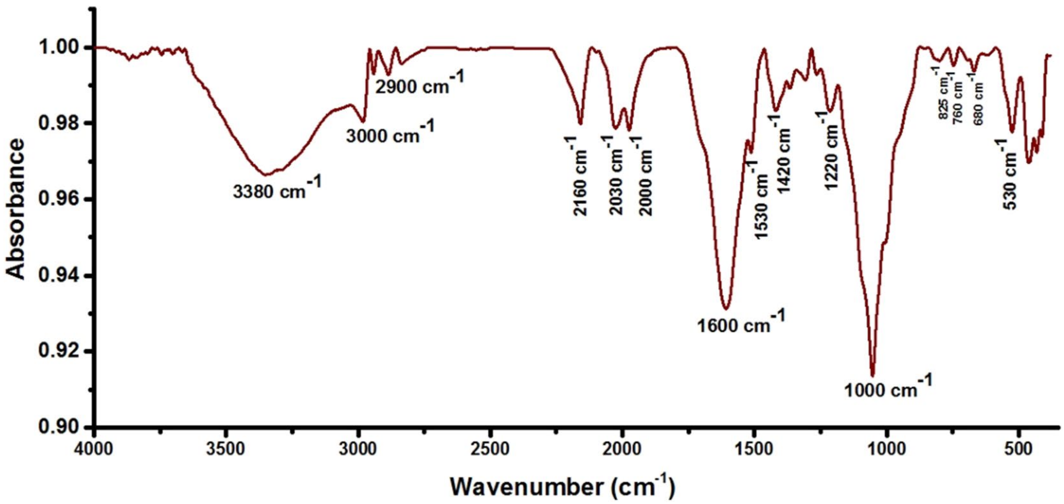

Fig. 1 FTIR of compost derived from chicken manure and cardboard

in the characteristic IR bands did not happen during composting, although a slight decrease and slight increase in the bands 3000 and 1420 cm^{-1} was observed, respectively.

The surface functional groups detected by IR, such as O–H, COOH, aromatic rings and NH_2 can play a significant role for attracting phenolic compounds from solution via different interaction mechanisms. Based on the earlier analysis, a schematic presentation of humic-rich compost is depicted in Fig. 2, along with the mechanisms of phenols interaction with the surface of compost.

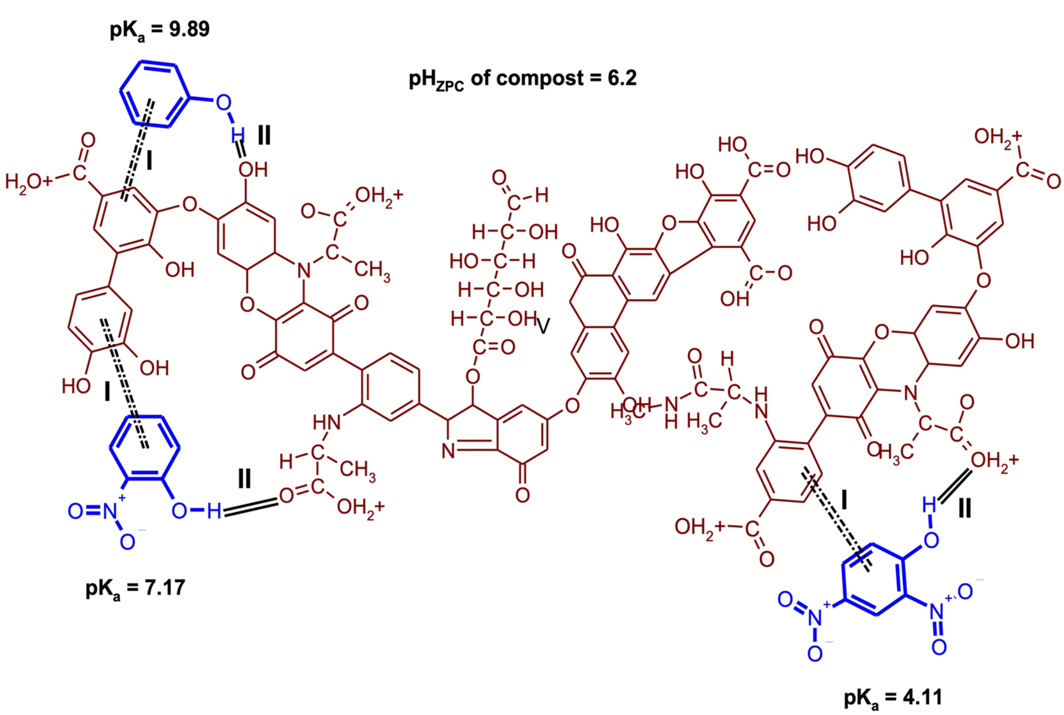

Fig. 2 Proposed structure of organic-rich compost and interaction mechanisms with phenols at pH 2.0. (**I**) π-π forces (**II**) H-boding

Finally, another important issue to be addressed before using compost as an adsorbent is the level of toxic metals in its matrix. Toxicity of compost is dependent on the bioavailable and leachable forms of heavy metals rather than the total concentration. The results of the leaching test indicated that the eluted levels of Cr, Pb, Cd, Zn, and Cu from compost were 1.3, 1.8, 1.9, 23.6, and 45.4 mg L^{-1}, respectively. The regulated TCLP limits for toxicity are 1.0 mg L^{-1} for Cd and 5.0 mg L^{-1} for Cr and Pb, while none are for Cu or Zn (Al-Saqarat et al., 2017). Therefore, the bioavailable concentration of toxic heavy metals was negligible and lower than the regulated limits for the TCLP test. Thus, the prepared compost, with a negligible concentration of bioavailable forms of heavy metals, is safe for adsorption use. Adding cardboard as a bulking agent had improved the overall composting process due to the following reasons: a) carbon-rich cardboard balanced nitrogen-rich chicken manure, b) the bulking agent absorbed excess moisture in the manure, and c) adding dry and shredded cardboard created air pockets in the pile and this accelerated the biodegradation process.

3.2 Adsorption Studies

3.2.1 Optimization of Adsorption Factors for Phenols Uptake

The effects of compost dosage, pH, contact time, and temperature on adsorption of the three adsorbates by compost are presented in Fig. 3. For comparison purposes, the optimum adsorption factors or parameters for phenol and other nitro-derivatives uptake by different adsorbents from the literature are compiled in Table 5 and summarized in Fig. 4.

Dosage of Compost The effect of mass on solutes uptake was examined over a wide range of 2.0–8.0 g L^{-1}, as shown in Fig. 3A. The removal of solutes was notably improved when the dose of adsorbent was increased from 2.0 to 6.0 g L^{-1}, but not at higher levels. The increasing removal with adsorbent dosage is attributed to the increase in the active sites and available surface area for adsorption, whereas at higher doses, aggregation of the active sites can lead to a reduction in the surface area (Almahbashiet al., 2023). At 6.0 g L^{-1}, the removal percentages were

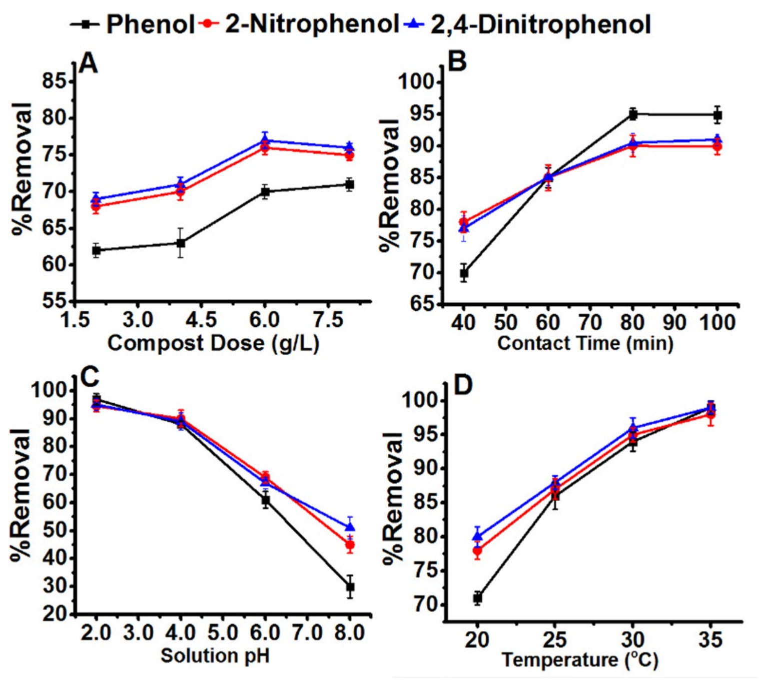

Fig. 3 Effect of different experimental conditions on phenols uptake by compost at 100 mg L^{-1} concentration. **A** Dosage – pH 2.0, contact time 80 min and temperature 25 °C. **B** Solution pH – dose 6.0 g L^{-1}, contact time 80 min, and temperature 25 °C. **C** Contact time – pH 2.0, dose 6.0 g L^{-1}, and temperature 25 °C. **D** Temperature – pH 2.0, dose 6.0 g L^{-1}, and contact time 80 min

Table 5 Reported equilibrium isotherm parameters for phenols uptake by different adsorbents

Adsorbent	Adsorbate	Model/ Shape[a,b]	Optimal conditions[c]			Q_{max} (mg/g)	Ref
			Dose (g/L)	pH	Equil. Time (min)		
Rice straw	Phenol	LM	20.0	-	180	6.0	Sarker and Fakhruddin (2017)
Zeolite	Phenol	L2/LM	20.0	4.0	60	160.0	Khalid et al. (2004)
Clay composite	Phenol	L1/LM	2.5	2.0	100	1665.0	Adebayo and Areo (2021)
Cclay composite	4-nitrophenol	L1/LM	2.5	7.0	100	477.0	Adebayo and Areo (2021)
MOFs	Phenol	C/LM	6.0	-	180	758.0	Liu et al. (2014)
MOFs	4-Nitrophenol	L2/LM	6.0	-	180	192.0	Liu et al. (2014)
Rice stalk-AC	Phenol	LM	1.0	7.0	150	70.0	Almahbashi et al. (2023)
Silica/calcium alginate nanocomposite	Phenol	L2/LM	4.0	7.0	140	101.0	Khoj (2024)
Zirconium-ferrite nanoparticles	Phenol	LM	6.0	2.0	140	334.0	Ali et al. (2020)
Zirconium-ferrite nanoparticles	2-Nitrophenol	LM	6.0	2.0	140	375.0	Ali et al. (2020)
Activated carbon	Phenol	L2/LM	2.0	6.0	250	142.0	Gundogdu et al. (2012)
β-cyclodextrin	2,4-dinitrophenol	LM	2.5	2.0	40	80.0	Mamman et al. (2023)
Pine Bark	Phenol	LM	4.0	6.0	120	143.0	Nadavala et al. (2014)
Activated carbon	Phenol	-	1.0	2.0	-	55.0	Vasiljević et al. (2006)
Activated carbon	2,4-dinitrophenol	-	1.0	2.0	-	90.0	Vasiljević et al. (2006)
Y zeolite	Phenol	L2/LM	5.0	2.0	200	170.0	El-Kordy et al. (2022)
Modified-Magadiite	Phenol	L2/LM	1.0	12.0	60	60.0	Ge et al. (2019)
$MgCl_2$-AC	Phenol	L2/LM	3.0	2.0	150	44.0	Hamadneh et al. (2020)
$MgCl_2$-AC	4-nitrophenol	L2/LM	3.0	2.0	150	122.0	Hamadneh et al. (2020)
Activated carbon	Phenol	L2/LM	1.0	-	120	177.0	Chaudhary et al. (2022)
Activated carbon	2-nitrophenol	L2/LM	1.0	-	120	308.0	Chaudhary et al. (2022)
Activated carbon	4-nitrophenol	L2/LM	1.0	-	120	292.0	Chaudhary et al. (2022)
Sewage sludge	Phenol	L2/LM	5.0	2.0	80	26.0	Bousba and Meniai (2014)
Char-tire	Phenol	L2/LM	1.0	2.0	150	17.0	Kusmierek and Swiatkowski (2023)
Pine cone	Phenol	LM	3.0	2.0	200	67.0	Bouchareb et al. (2019)
Compost	Phenol	L2/LM	6.0	2.0	80	115.0	This study
Compost	2-nitrophenol	L2/LM	6.0	2.0	80	128.0	This study
Compost	2,4-dinitrophenol	L2/LM	6.0	2.0	80	137.0	This study

[a]Classification of isotherms was made according to Giles et al. (1974)

[b]LM: Langmuir model

[c]The conditions for equilibrium isotherm. In most cases, adsorbate concentration varied over the range 5–500 mg L^{-1}

69, 76, and 77 for Ph, 2-NPh, and 2,4-DNPh, respectively. The observed optimum dosage for compost, 6.0 g L^{-1}, is in the range of other studies in the literature, where doses in the range 1.0–20 g L^{-1} have been employed for removal with activated carbon, non-conventional adsorbents and nanocomposites (Fig. 4A). Many adsorbents are effective for removing phenol and nitro-derivatives at low dosages. For instance, optimum removal was reported at 1.0 g L^{-1} using activated carbon (Chaudhary et al., 2022), at 3.0 g L^{-1} using methacrylic acid-β-cyclodextrin (Mamman et al., 2023), at 4.0 g L^{-1} by silica/alginate nanocomposite (Khoj, 2024), 5.0 g L^{-1} using pine bark (Nadavala et al., 2014), or at 6.0 g L^{-1} using zirconium-ferrite nanoparticles (Ali et al., 2020). Relatively higher doses, such as 12.0 g L^{-1}

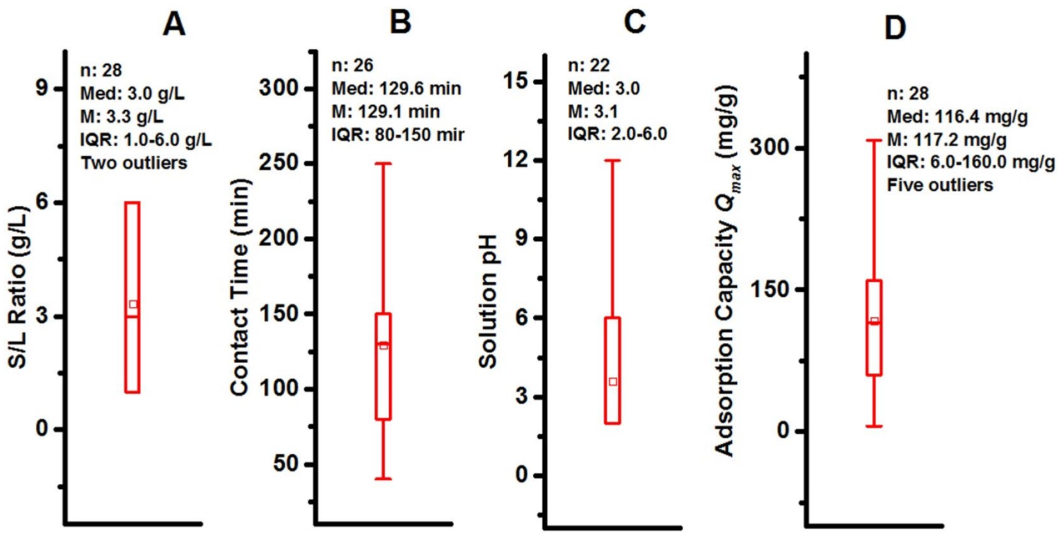

Fig. 4 Adsorption parameters of phenol and nitro-derivatives by different adsorbents presented by box-whisker plot. **A** Optimum dosage, **B** Optimum equilibrium time, **C** Solution pH, and **D** Maximum adsorption capacity. The horizontal lines in the box indicate the median value, red squares indicate the mean value, the length of the box indicates the interquartile range IQR, and the whiskers indicate the range of typical values

for surfactant-modified alumina (Adaka & Pal, 2006) or 20.0 g L^{-1} for rice raw and zeolite have also been reported, but these may reduce practical application (Khalid et al., 2004; Sarker & Fakhruddin, 2017).

Contact Time The effect of contact time on phenols uptake is presented in Fig. 3B. Fast removal of the solutes was observed during the first hour of the process and almost unchanged after 80 min of interaction, which would be the equilibrium time of the uptake. In most studies in the literature, uptake of phenols occurs rapidly at the very first few minutes of interaction and then proceeds gradually until equilibrium is attained at variable equilibrium times between 40–250 min, as summarized in Table 4 and Fig. 4B. Median, mean, and IQR of the collected results were 129.6, 129.1, and 80–150 min, respectively, and differences among adsorbents were attributed to their textural properties (Gundogdu et al., 2012; Hamadneh et al., 2020; Mamman et al., 2023). The shortest equilibrium time was reported for 2,4-DNPh removal using magnetic methacrylic acid-β-cyclodextrin, at only 40 min (Mamman et al., 2023). Equilibrium for Ph was attained in 60 min by modified Magadiite (Ge et al., 2019), in 100 min by zeolite (El-Kordy et al., 2022), and after 150 and 200 min using $MgCl_2$-impregnated activated carbons and activated carbon, respectively (Gundogdu et al., 2012; Hamadneh et al., 2020). Maximum removal of Ph and 2-nitrophenol by zirconium-ferrite nanoparticles was attained in 120 min (Ali et al., 2020). Thus, the equilibrium time for phenols uptake using compost was relatively short when compared to other adsorbents.

Solution pH and Adsorption Mechanisms As shown in Fig. 3C, pH had a significant influence on phenols uptake from solution, the removal of the three adsorbates being reduced from 95% down to 30–50% as pH increased from 2.0 to 8.0. Solution pH controls the acid/base equilibrium of adsorbate and the net surface charge of the adsorbent. Over the pH range 2.0–8.0 studied here, both Ph (pK_a 9.89) and 2-NPh (pK_a 7.17) will be in their neutral forms. For 2,4-DNPh (pK_a 4.11), the adsorbate will be negatively charged over the range 5.0–8.0. The estimated point of zero charge pH_{ZPC} of prepared compost was measured at 6.3. Accordingly, at a solution pH > 6.3, the net surface charge of compost is negative while positive at pH < 8.2 (Al-Zawahreh et al., 2022). Thus, the favorable uptake of phenolic compounds in an acidic medium can be attributed to the strong interaction between the positively charged surface and the π-aromatic system in the three solutes. Moreover, the protonated surface at acidic pH can also enhance the

H-bonding with phenolic compounds. In the case of 2,4-DNPh, electrostatic repulsion between negatively charged adsorbent and the anionic form of the adsorbate at alkaline pH will also reduce adsorption.

In agreement with our results, most studies report higher removal of phenol and nitro-derivatives at acidic medium, as summarized in Table 5 and Fig. 4C. For example, a pH of 2 has been reported as optimal for the removal of phenol on zirconium-ferrite nanoparticles (Ali et al., 2020), on zeolite (El-Kordy et al., 2022), or for phenol and 2,4-DNPh on activated carbon (Vasiljević et al., 2006). The generally more favorable uptake of phenol and related derivatives at pH 2.0 supports the hypothesis that the adsorbates were adsorbed on the surface mainly through dispersion forces between π electrons in phenol's aromatic ring and π electrons of humic/fulvic acid in compost. In addition, electrostatic attraction forces were present but less dominant in the uptake process. Under acidic conditions, only non-electrostatic interactions such as π–π interactions and donor–acceptor interactions can promote the adsorption of phenol on compost, with a potential contribution from H-bond interactions (Fig. 2).

Temperature As shown in Fig. 3D, increasing temperature over the range 20–35 °C had a positive and significant effect on adsorbate removal from solution, which improved from 70–80 up to ~ 100%. The improved uptake of solutes at higher temperature reflects the endothermic nature of the process. In the literature, mixed results have been reported for the effect of temperature on phenols uptake from solution, with both exo- and endothermic processes reported (Bousba & Meniai, 2014; Chaudhary et al., 2022). For example, removal of phenol by zeolite (El-Kordy et al., 2022) or removal of Ph and 2-NPh using activated carbon (Chaudhary et al., 2022) were found to be endothermic, while removal of Ph and 2-NPh using zirconium-ferrite nanoparticles (Ali et al., 2020) or phenol using sewage sludge (Bousba & Meniai, 2014) were reported to be exothermic processes. The endothermic nature of the process can be explained by several factors (Bousba & Meniai, 2014; El-Kordy et al., 2022); (a) the increase of the temperature can facilitate the diffusion of the adsorbed phenolic molecules towards the internal pores of the adsorbent by decreasing the viscosity of the solution; (b) phenol and nitro-phenols can form H-bonds which are broken at high temperature resulting in their higher removal from solution; (c) the increase in the temperature can improve the capacity of the adsorbent due to an increase in the swelling of the active sites to allow more available sites for the phenolic compounds; and (d) polymerization reaction of phenols enhanced at higher temperature.

3.2.2 Kinetics of Phenols Adsorption by Compost

The results of the kinetics tests are presented in Fig. 5 with model parameters summarized in Table 6. Reaction-based models including first and second order models were more adequate to present kinetic

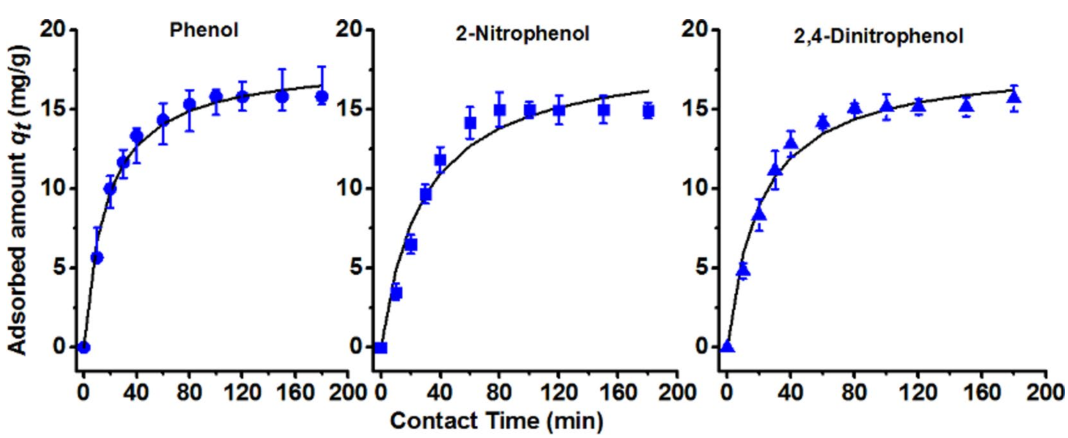

Fig. 5 Kinetic profiles for phenols uptake by compost. Conditions: pH 2.0, phenols level 100 mg/L. compost dose 6.0 g/L, and temperature 25 °C. Lines present first order fitting for the experimental results (ARE 2.0–4.6)

Table 6 Parameters of different models for adsorption kinetics of phenols on compost[a]

Solute	q_e(exp)	First-order				Second order				
		k_1	q_e(model)	ARE	R^2	k_2	q_e(model)	h^b	ARE	R^2
Ph	15.8	$0.047\pm0.002^{***}$	$15.7\pm0.2^{***}$	3.0	0.997	$0.0026\pm0.0003^{***}$	$15.3\pm0.1^{***}$	0.61	2.1	0.999
2-NPh	15.0	$0.029\pm0.003^{***}$	$16.6\pm0.7^{***}$	6.3	0.990	$0.0010\pm0.0005^{***}$	$15.5\pm0.4^{***}$	0.24	4.6	0.998
2,4-DNPh	15.2	$0.034\pm0.002^{***}$	$15.7\pm0.2^{***}$	4.4	0.998	$0.0019\pm0.0006^{***}$	$14.9\pm0.2^{***}$	0.42	2.0	0.998

[a]The background of all adopted models is provided in Table S2 (Supplementary Material Eqs S4-S6)

[b]Initial uptake rate $h(mgg^{-1}min^{-1}) = k_2 q_e^2$

Average relative error (ARE) is estimated as outlined in Eq S10 in Supplementary Material

Significance of parameter estimations is indicated as follows: *significant at a P-value of 0.05; **significant at a P-value of 0.01; ***significant at a P-value of 0.001

data compared to diffusion-based models. As shown in Table 6, the best results were achieved using pseudo-first order model with ARE 2.0–4.6. The inadequacy of intraparticle diffusion model indicates that reaction of phenols with the surface controlled the process while diffusion inside the pores of compost had a much lower effect on the entire process. Based on the pseudo-second order model, the initial reaction rates for adsorption were 0.52 mg g^{-1} min^{-1} for 2-NPh, 0.75 mg g^{-1} min^{-1} for 2,4-DNPh, and 0.97 mg g^{-1} min^{-1} for Ph. The initial adsorption rate *h* was taken as a guide to compare uptake rates of phenol and nitro-derivatives over different adsorbents (Fig. 6). In some cases, *h* was provided in the study, and in other cases, *h* was estimated from the reported parameters of the model. As shown in Fig. 6, many of the examined adsorbents presented high adsorption rates for phenols, in general higher than the values obtained in this study for compost. For example, values of 7.58 mg g^{-1} min^{-1}, 3.74 mg g^{-1} min^{-1}, 2.43 mg g^{-1} min^{-1}, and 1.83 mg g^{-1} min^{-1} have been reported for adsorption of phenol on pine bark, silica-calcium alginate nanocomposite, MOFs, and $MgCl_2$-activated carbon, respectively (Hamadneh et al., 2020; Khoj, 2024; Liu et al., 2014; Nadavala et al., 2014). The highest rate was reported for 2,4-DNPh uptake by β-cyclodextrin with a value of 11.34 mg g^{-1} min^{-1} (Mamman et al., 2023). In some cases, lower uptake rates have been reported, such as Ph and 2-NPh on lignin activated carbon, with values estimated at 0.17 and 0.38 mg g^{-1} min^{-1}, respectively (Chaudhary et al., 2022).

3.2.3 Equilibrium Adsorption

The equilibrium adsorption curves are displayed in Fig. 7 while the parameters of different models are summarized in Table 7. The shape of the curves is L2 according to Giles classification, which indicates low competition of solutes with solvent molecules and

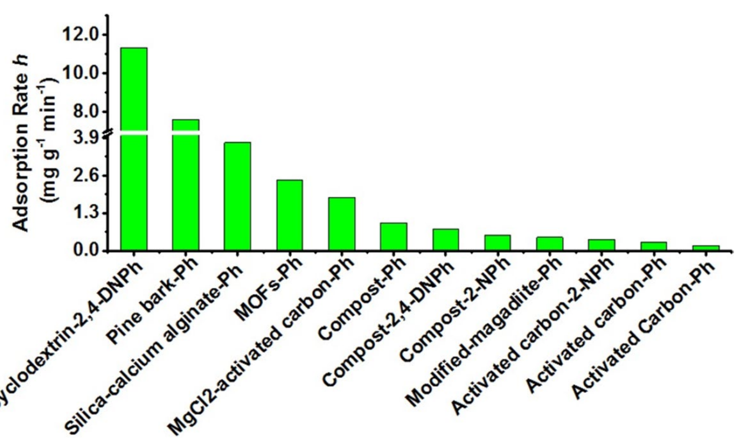

Fig. 6 Estimated adsorption rate of phenol and nitro-derivatives for compost and other adsorbents (Ph: Phenol, 2-NPh: 2-nitrophenol, 2,4-DNPh: 2,4-dinitrophenol)

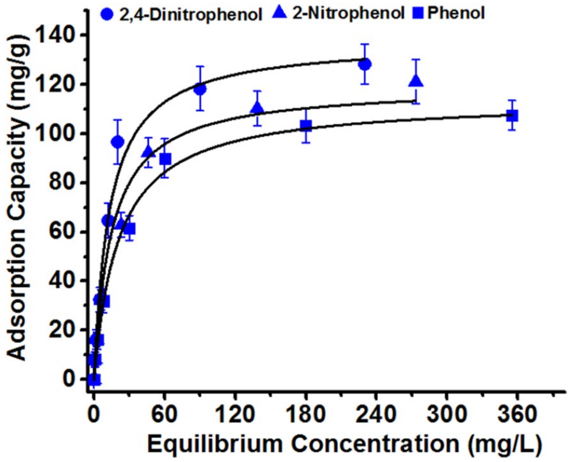

Fig. 7 Equilibrium isotherms of phenols adsorption by compost. Conditions: pH 2.0, compost dose 6.0 g/L, temperature 25 °C, and 100 min contact time. Lines present Langmuir fitting for the experimental data (ARE 4.3–6.7%)

adsorption proceed until surface saturation (Giles et al., 1974). Although Redlich-Peterson model was appropriate in representing adsorption results with ARE 4.0–5.8, this model did not give good prediction of Q_{max} for phenols. As known, the ratio K_{RP}/A_{RP} should be close to experimental Q_{max} values, and this was not achieved. Freundlich model was not suitable for presenting adsorption data with ARE 14.9–20.2, indicating that the surface of compost is homogeneous with equal-energy active sites. However, the model indicated better affinity of nitro-phenols compared to phenol, as shown by the magnitude of K_F (Table 6). The best model was Langmuir with ARE 4.3–6.7 and predicted Q_{max} values close to experimental ones (Table 7).

According to the Langmuir model, the adsorption capacity of adsorbates increased in the sequence Ph < 2-NPh < 2,4-DNPh. The maximum adsorption capacity of the compost for phenols was 115.25 mg g^{-1} for Ph, 128.47 mg g^{-1} for 2-NPh, and 136.68 mg g^{-1} for 2,4-DNPh. K_L, the energy parameter of the model, indicated the higher uptake for 2,4-DNPh, with a value of 0.082 L mg g^{-1}. In agreement with our results, a better removal of nitro-phenols compared to phenol was reported using zirconium-ferrite nanoparticles (Ali et al., 2020), activated carbon (Vasiljević et al., 2006) and $MgCl_2$-activated carbon (Chaudhary et al., 2022; Hamadneh et al., 2020). The higher adsorption capacity for nitro-phenols compared to phenols can be attributed to the following reasons: (a) the solubility of phenol in water is 17 and 47 times higher than that of 2,4-DNPh and 2-NPh, respectively, and both 2,4-DNPh and 2-NPh

Table 7 Parameters of different models for equilibrium adsorption of phenols by compost[a]

Langmuir						
Adsorbate	Q_{max} (exp) (mg/g)		Q_{max} (mg/g)	K_L	ARE[b]	R^2
Ph	111.0		115.2 ± 0.4	0.047 ± 0.005	4.5	0.989
2-NPh	125.0		128.4 ± 0.3	0.049 ± 0.006	4.3	0.991
2,4-DNPh	134.0		137.0 ± 0.2	0.082 ± 0.005	6.7	0.994
Freundlich						
Adsorbate	K_F			n_F	ARE	R^2
Ph	19.8 ± 1.1			3.25 ± 0.6	16.2	0.882
2-NPh	20.7 ± 2.2			3.03 ± 0.5	14.9	0.891
2,4-DNPh	27.5 ± 1.7			3.31 ± 0.9	20.2	0.911
Redlich-Peterson						
Adsorbate	K_{RP}	a_{RP}	g	K_{RP}/A_{RP}	ARE	R^2
Ph	5.00 ± 0.04	0.037 ± 0.003	1.02 ± 0.02	135.14	4.5	0.988
2-NPh	7.31 ± 0.06	0.074 ± 0.004	0.95 ± 0.01	98.78	4.0	0.991
2,4-DNPh	9.36 ± 0.03	0.042 ± 0.006	1.09 ± 0.04	222.86	5.8	0.995

[a]The background of the adopted isotherms and the physical meaning of all parameters are provided in Table S2 (Supplementary Material Eqs S7-S9)

[b]Average relative error is estimated as outlined in Eq S10 in Supplementary Material

have higher partition coefficients compared to Ph (Table S1), what will reduce phenol affinity toward the surface and will increase the interaction of nitrophenols with organic-rich compost; (b) the presence of nitro groups in the phenols increases their interaction with the compost surface via H-bonding forces (Fig. 2).

3.3 Comparison of Compost to other Adsorbents

3.3.1 Q_{max} Criterium

As stated previously, while many research studies have examined the performance of different adsorbents toward phenolic compounds (Almahbashi et al., 2023; Hamadneh et al., 2020; Ho, 2022; Liu et al., 2014), there is no available research studies on using compost for removing phenol and nitro-derivatives. Among the parameters obtained in adsorption studies, Q_{max} is the best indicator to compare the performance of different adsorbents toward pollutants (Al-Zawahreh, 2025; Al-Zawahreh et al., 2024b). The Q_{max} values collected here from the literature are presented in Table 5 and summarized in Fig. 4D. The median, mean, and IQR of the collected results were 116.4 mg g^{-1} for Ph, 117.2 mg g^{-1} for 2-NPh, and 6.0–160.0 mg g^{-1} for 2,4-DNPh. Outstanding performance in this sense has been reported for zirconium-ferrite nanoparticles toward Ph and 2-NPh with capacities of 334.0 and 375.0 mg g^{-1}, respectively (Ali et al., 2020), and of *Cocos nucifera*-clay composite for removing Ph (1665.0 mg g^{-1}) and 4-NPh (477.0 mg g^{-1}) (Adebayo & Areo, 2021).

As shown in Fig. 8, which represents the maximum uptake of phenol and nitro-derivatives for different adsorbents along with compost, both *Cocos nucifera*-clay composite and metal – organic frameworks manifested a high retention capacity for Ph, 750–1600 mg g^{-1}. Biosorbents including pine bark, natural zeolite, synthetic zeolite and activated carbon are relatively good adsorbents for Ph, whereas other adsorbents used in these studies (sewage sludge, modified-magadiite, pinecone, rice straw, char tire, and certain activated carbons) presented low adsorption capacity, below 100 mg g^{-1}, which may hinder their utilization for real wastewater treatment units (Bouchareb et al., 2019; Kusmierek & Swiatkowski, 2023). Regarding nitro-derivatives of phenol, activated carbon, nano-zirconium-ferrite, and *Cocos nucifera*-clay composite presented the best performance, with maximum adsorption capacity reaching 290–470 mg g^{-1} for 2-NPh and

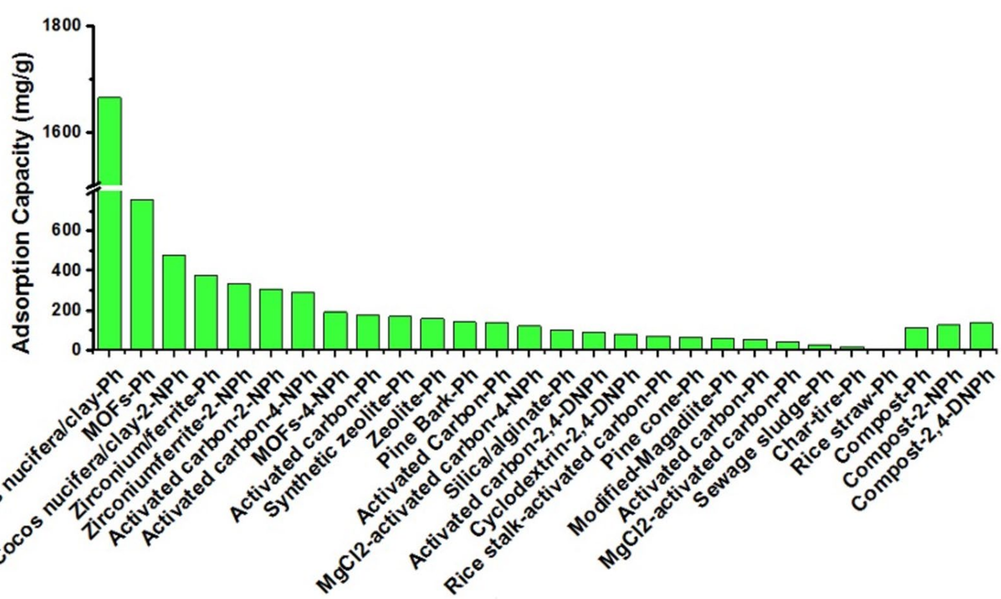

Fig. 8 Maximum adsorption capacity of phenol and nitro-derivatives reported for different adsorbents and compost. (Ph: Phenol, 2-NPh: 2-nitrophenol, 4-NPh: 4-nitrophenol, 2,4-DNPh: 2,4-dinitrophenol)

4-NPh. The performance of $MgCl_2$-activated carbon and MOFs was also promising for 4-NPh (120 and 190 mg g^{-1}, respectively). The performance of compost as bioadsorbent for phenols is competitive with literature reports, since its uptake capacity (115–137 mg g^{-1}) was higher than some activated carbons, rice straw, sewage sludge, modified-magadiite, and $MgCl_2$-activated carbon. Due to its low production cost, there is no urgent need for its recycling like other expensive adsorbents like activated carbon, MOFs, zeolite, and nanomaterials.

3.3.2 Production Cost and Adsorbent Cost Index

The assessment of the overall performance of adsorbents needs considering also their average production costs, in order to find out the most-cost effective, as this is one of the principal considerations and obstacles to commercializing adsorption technology, i.e., scaling up adsorption technologies from pilot to industrial scale. In this sense, it has been proposed in the literature that the production cost of "low-cost adsorbents" should be less than 1.0 USD kg^{-1}, "moderate-cost adsorbents" should be 3.0–6.0 USD kg^{-1}, and "high-cost adsorbents" could cost up to 15.0–20.0 USD kg^{-1} (Kumar et al., 2019). As summarized in Table 4, expensive adsorbents used for removal of phenol from water include activated carbon, metal – organic frameworks, zirconium-ferrite nanoparticles, β-cyclodextrin, and synthetic zeolite. Low-cost natural/industrial and bio-adsorbents include zeolite, rice straw, clay composite, silica, sewage sludge, and compost.

Researchers rarely refer to the production cost of their adsorbents, as well as the additional costs of the treatment process, likely due to the lack of a unified or standardized procedure to estimate these expenses (GadelHak et al., 2023). In this section, the cost of utilizing different adsorbents to remove phenol based solely on their production costs will be addressed. The expenses of the adsorption process itself, such as heating, stirring, filtration, and the additional costs of running fixed bed technology, were not considered. For instance, the net production cost of an adsorbent can be estimated from the following costs: cost of raw materials, cost of raw materials transportation, cost of the chemicals consumed, cost of consumed energy, cost of mixing, cost of heating, cost of filtration, and cost of grinding (GadelHak et al., 2023).

Based on our search, there is no comprehensive review related to the production and utilization costs of synthetic and nonconventional adsorbents, despite the decades of intensive research in this field. However, a few studies reported approximate production costs of activated carbon (Samrane & Bouhaouss, 2022), multiwalled carbon tubes (Gkika et al., 2022), metallic nanoparticles (Huaxu et al., 2020), metal – organic frameworks (Sharanyakanth & Radhakrishnan, 2020), synthetic zeolite and natural zeolites (GadelHak et al., 2023). As shown in Table 8, activated carbon, metal – organic frameworks, nanoparticles, and other synthetic adsorbents have high production costs, which are attributed to the usage of expensive chemicals as well as the use of high energy expenditures during the manufacturing process (GadelHak et al., 2023). The substantial cost disparity within the prices of synthetic adsorbents was traced back to differences in the cost of electricity, chemicals, the value of manufacturing taxes, and labor wage in the countries that produce these nano-adsorbents (GadelHak et al., 2023). Although metal–organic frameworks and zirconium-ferrite nanoparticles outperformed other adsorbents for removing phenol, their application on a large scale is a questionable issue considering their high production costs, which cost up to 7.0–37.0 USD g^{-1}. Among adsorbents, cocos nucifera-clay composite has shown an excellent capacity for phenol and an average production cost of 0.1 USD kg^{-1}. Compost has a much lower production cost than other adsorbents (Al-Zawahreh & Paradelo, 2025), which is related to the low cost of feedstocks, as well as the absence of heating or chemical additions during the preparation process. In terms of compost production costs, most of the expenses were related to the salary of workers who turn compost piles regularly, as well as the cost of various compost analyses and sieving. The production cost of compost was calculated to be 0.04 USD kg^{-1} (Al-Zawahreh et al., 2024a).

However, comparing the production costs of different adsorbents based on their unit mass would be misleading considering the high variations in their uptake capacities for phenol. Thus, estimated costs should be normalized for comparison of adsorbents per adsorption capacity rather than per unit mass. This can be simply done by dividing the cost per g adsorbent (e.g., USD/$g_{adsorbent}$) by the adsorption capacity of the adsorbent to obtain the cost in units of USD/$g_{adsorbate}$

Table 8 Production cost and cost index for removing 1.0 g phenol for different adsorbents

Adsorbent	Production cost (USD/kg)[a]	Adsorption capacity Q_{max} (mg/g)[b]	Cost index (USD/g_{phenol})[c]	Cost index (US Cent/g_{phenol})[c]
Y zeolite	2.5	170.0	0.015	1.471
Activated carbon	1.25	55.0	0.023	2.273
Activated carbon	1.25	177.0	0.007	0.706
Activated carbon	1.25	142.0	0.009	0.880
Activated carbon	1.25	70.0	0.018	1.786
Activated carbon	1.25	44.0	0.028	2.841
Clay composites	0.10	1665.0	0.000	0.006
Zeolite	0.12	160.0	0.001	0.075
Compost	0.04	115.0	0.000	0.035

[a]The average production costs of the adsorbents were collected from a recent review article (GadelHak et al., 2023)

[b]Uptake capacities of phenol by different adsorbents were collected from Table 5

[c]Cost index was estimated from Eq. 1. Before using Eq. 1, production cost of the adsorbent and adsorbent capacity was expressed as $USD/g_{adsorbent}$ and $g_{adsorbate}/g_{adsorbent}$, respectively. USD = 100 Cents

(Ighalo et al., 2022). The cost of adsorbent per gram of adsorbate, also known as cost index of adsorbent, can be used to determine the cost of the adsorption process and estimated as follows (Al-Zawahreh & Paradelo, 2025; Ighalo et al., 2022):

$$AdsorbentCostIndex\left(\frac{USD}{g_{adsorbate}}\right) = \left[\frac{ProductionCost(\frac{USD}{g_{adsorbent}})}{Qmax\left(\frac{g_{adsorbate}}{g_{adsorbent}}\right)}\right]$$

As summarized in Table 8, the cost index for removing 1.0 g phenol was relatively high using activated carbons, which range from 0.007 up to 0.028 USD. The high cost index of activated carbon is attributed to the high production cost of this material, which involves high consumption of energy. In addition to activated carbon, the cost index of synthetic zeolite, Y zeolite, was rather high and estimated at 0.115 USD/g_{phenol}, as summarized in Table 8. On the other hand, the cost index estimated for natural zeolite was promising, estimated at 0.001 USD. Interestingly, the lowest cost index was estimated for clay with a value down to 0.006 US Cent/g_{phenol}, and this is attributed to the unusual adsorption capacity of this adsorbent for phenol, 1665.0 mg/g, as summarized in Table 8. The estimated cost index of compost for removing 1.0 g phenol was 0.035 US Cent, and this is very promising compared to activated carbon and synthetic zeolite. With an adsorption capacity of 115.0–136 mg/g and a production cost of 0.04 USD/kg, compost is a practical adsorbent for removing Ph, 2-NPh, and 2,4-DNPh as addressed in this work. Recycling of compost seems unnecessary considering its modest production cost.

4 Conclusions

Compost derived from chicken manure and cardboard as a bulking agent is a promising bioadsorbent for removing weakly interacting phenolic compounds from water. The prepared compost was safe, stable, mature, and rich in humic/fulvic fractions, and it outperformed many of non-conventional and synthetic adsorbents toward phenol and related nitro derivatives. Equilibrium studies indicated that compost can adsorb 110–130 mg g^{-1} of phenol and its nitro-derivatives. Although activated carbon and synthetic zeolite manifested a high adsorption for phenol, their application on a large scale may not be feasible considering their high "adsorbent cost index": 1.5–2.8 US Cent to remove 1.0 phenol from solution. The estimated "adsorbent cost index" of compost was 0.035 US Cent to remove 1.0 g phenol. Recycling of compost was not examined due to its low production cost, 0.04 USD kg^{-1}. Moreover, exhausted compost can be used as a feedstock for another composting cycle.

Authors Contribution Khaled Al-Zawahreh: Writing – review & editing, Writing – original draft, Visualization, Validation, Conceptualization Project administration, Methodology, Formal analysis, Data curation. Remigio Paradelo: Writing – review & editing, Validation, Methodology.

Funding Open Access funding provided thanks to the CRUE-CSIC agreement with Springer Nature.

Data Availability Data will be made available on reasonable request.

Declarations

Ethics Approval Not applicable.

Consent for Publication Not applicable.

Competing Interests The authors declare that they have no conflict of interest.

References

Abolhassani, M., Derafshi, M., Hassani, A., et al. (2023). Impacts of the application of enrofloxacin-containing poultry manure on the soil microbial activities. *Environmental Processes, 10*, Article 30. https://doi.org/10.1007/s40710-023-00645-8

Adaka, A., & Pal, A. (2006). Removal of phenol from aquatic environment by SDS-modified alumina: Batch and fixed bed studies. *Separation and Purification Technology, 50*, 256–262. https://doi.org/10.1016/j.seppur.2005.11.033

Adebayo, M., & Areo, F. (2021). Removal of phenol and 4-nitrophenol from wastewater using a composite prepared from clay and *cocos nucifera* shell: Kinetic, equilibrium and thermodynamic studies. *Resources, Environment and Sustainability, 3*, Article 100020. https://doi.org/10.1016/j.resenv.2021.100020

Ahmad, I., Akhtar, M., Jadoon, I., et al. (2017). Equilibrium modeling of cadmium biosorption from aqueous solution by compost. *Environmental Science and Pollution Research, 24*, 5277–5284. https://doi.org/10.1007/s11356-016-8280-y

Ahmaruzzaman, M. S., & Gadore, V. (2024). Phenolic compounds in water: From toxicity and source to sustainable solutions – An integrated review of removal methods, advanced technologies, cost analysis, and future prospects. *Journal of Environmental Chemical Engineering, 12*, Article 112964. https://doi.org/10.1016/j.jece.2024.112964

Ahn, H., Richard, L., & Choi, H. (2007). Mass and thermal balance during composting of a poultry manure–wood shavings mixture at different aeration rates. *Process Biochemistry, 42*, 215–223. https://doi.org/10.1016/j.procbio.2006.08.005

Albadarin, A., & Al-Zawahreh, K. (2025). Selection guide for high performance carbon adsorbents for phenol: An overview. *Research on Chemical Intermediates, 51*, 6655–6690. https://doi.org/10.1007/s11164-025-05780-5

Albrecht, R., Le Petit, J., Terrom, G., et al. (2011). Comparison between UV spectroscopy and NIRS to assess humification process during sewage sludge and green wastes co-composting. *Bioresource Technology, 102*, 4495–4500. https://doi.org/10.1016/j.biortech.2010.12.053

Ali, S., Arya, M., Abul Kalam Al-Sehemi, A., et al. (2020). Adsorption potential of zirconium-ferrite nanoparticles for phenol, 2-chlorophenol and 2-nitrophenol: Thermodynamic and kinetic studies. *Desalination and Water Treatment, 179*, 183–196. https://doi.org/10.5004/dwt.2020.25039

Almahbashi, N., Kutty, S., Jagaba, A., et al. (2023). Phenol removal from aqueous solutions using rice stalk-derived activated carbon: Equilibrium, kinetics, and thermodynamics study. *Case Studies in Chemical and Environmental Engineering, 8*, Article 100471. https://doi.org/10.1016/j.cscee.2023.100471

Al-Saqarat, B. S., Ibrahim, K. M., Musleh, F. M., & Al-Degs, Y. S. (2017). Characterization and utilization of solid residues generated upon oil and heat production from carbonate-rich oil shale. *Environmental Earth Sciences, 76*(7), Article 264. https://doi.org/10.1007/s12665-017-6578-9

Al-Zawahreh, K. (2025). A screening guide for efficient acid dyes adsorbents. *Environmental Processes, 12*, Article 6. https://doi.org/10.1007/s40710-025-00746-6

Al-Zawahreh, K., & Paradelo, R. (2025). Assessment of micro and nanosize C-based adsorbents for methylene blue uptake: A review. *Desalination and Water Treatment, 321*, Article 100956. https://doi.org/10.1016/j.dwt.2024.100956

Al-Zawahreh, K., Barral, M. T., Al-Degs, Y., & Paradelo, R. (2021). Comparison of the sorption capacity of basic, acid, direct and reactive dyes by compost in batch conditions. *Journal of Environmental Management, 294*, Article 113005. https://doi.org/10.1016/j.jenvman.2021.113005

Al-Zawahreh, K., Al-Degs, Y., Barral, M. T., & Paradelo, R. (2022). Optimization of Direct Blue 71 sorption by organic rich-compost following multilevel multifactor experimental design. *Arabian Journal of Chemistry, 15*, Article 103468. https://doi.org/10.1016/j.arabjc.2021.103468

Al-Zawahreh, K., Barral, M. T., & Paradelo, R. (2024a). Assessment of batch and fixed bed processes for competitive removal of Direct Dyes by a Grade III Compost

Adsorbent: Relative Efficacy Factor. *Water, Air, and Soil Pollution, 235*, Article 604. https://doi.org/10.1007/s11270-024-07419-4

Al-Zawahreh, K., Barral, M. T., & Paradelo, R. (2024b). Overview of factors to take into account when selecting high-grade dye adsorbents. *Environmental Technology Reviews, 13*, 587–613. https://doi.org/10.1080/21622515.2024.2404650

Anastopoulos, I., & Kyzas, G. (2015). Composts as biosorbents for decontamination of various pollutants: A review. *Water, Air & Soil Pollution, 226*, Article 61. https://doi.org/10.1007/s11270-015-2345-2

Bampi, J., da Silva, T., da Luz, C., et al. (2024). Study of the competitive effect on the adsorption of phenol and 4-nitrophenol in a batch reactor and fixed-bed column using coconut shell activated carbon. *Journal of Water Process Engineering, 65*, Article 105825. https://doi.org/10.1016/j.jwpe.2024.105825

Barrington, S., Choinière, D., Trigui, M., et al. (2002). Effect of carbon source on compost nitrogen and carbon losses. *Bioresource Technology, 83*, 189–194.

Bernal, M., Alburquerque, J., & Moral, R. (2009). Composting of animal manures and chemical criteria for compost maturity assessment. A review. *Bioresource Technology, 100*, 5444–5453. https://doi.org/10.1016/j.biortech.2008.11.027

Biyada, S., Merzouki, M., Imtara, H., et al. (2019). Assessment of the maturity of textile waste compost and their capacity of fertilization. *European Journal of Scientific Research, 159*, 399–412.

Biyada, S., Merzouki, M., Elkarrach, K., & Benlemlih, M. (2020). Spectroscopic characterization of organic matter transformation during composting of textile solid waste using UV–Visible spectroscopy, Infrared spectroscopy and X-ray diffraction (XRD). *Microchemical Journal, 159*, Article 105314. https://doi.org/10.1016/j.microc.2020.105314

Bouchareb, S., Hank, D., Abdel Salam, M., et al. (2019). Adsorption of phenol onto alginate-adsorbent beads prepared from pine cone: Equilibrium and factorial design methodology. *Desalination and Water Treatment, 137*, 143–153. https://doi.org/10.5004/dwt.2019.23185

Bousba, S., & Meniai, A. (2014). Removal of phenol from water by adsorption onto sewage sludge based adsorbent. *Chemical Engineering Transactions, 40*, 235–240. https://doi.org/10.3303/CET1440040

Chaudhary, M., Suhas, Kushwaha, S., et al. (2022). Studies on the Removal of Phenol and Nitrophenols from Water by Activated Carbon Developed from Demineralized Kraft Lignin. *Agronomy, 12*, 2564. https://doi.org/10.3390/agronomy12102564

Dąbrowski, A., Podkościelny, P., Hubicki, Z., et al. (2005). Adsorption of phenolic compounds by activated carbon—a critical review. *Chemosphere, 58*, 1049–1070. https://doi.org/10.1016/j.chemosphere.2004.09.067

Ding, Z., Kheir, A., Ali, M., et al. (2020). The integrated effect of salinity, organic amendments, phosphorus fertilizers, and deficit irrigation on soil properties, phosphorus fractionation and wheat productivity. *Scientific Reports, 10*, Article 2736. https://doi.org/10.1038/s41598-020-59650-8

El Hajjouji, H., Fakharedine, N., Baddi, G., et al. (2007). Treatment of olive mill waste-water by aerobic biodegradation: An analytical study using gel permeation chromatography, ultraviolet–visible and Fourier transform infrared spectroscopy. *Bioresource Technology, 98*, 3513–3520. https://doi.org/10.1016/j.biortech.2006.11.033

El Ouaqoudi, F., El Fels, L., Lemée, L., et al. (2015). Evaluation of lignocelullose compost stability and maturity using spectroscopic (FTIR) and thermal (TGA/TDA) analysis. *Ecological Engineering, 75*, 217–222. https://doi.org/10.1016/j.ecoleng.2014.12.004

El-Kordy, A., Dehmani, Y., Douma, M., et al. (2022). Experimental study of phenol removal from aqueous solution by adsorption onto synthesized Faujasite-type Y zeolite. *Desalination & Water Treatment, 277*, 144–154. https://doi.org/10.5004/dwt.2022.28958

GadelHak, Y., El-Azazy, M., Shibl, M., et al. (2023). Cost estimation of synthesis and utilization of nano-adsorbents on the laboratory and industrial scales: A detailed review. *Science of the Total Environment, 875*, Article 162629. https://doi.org/10.1016/j.scitotenv.2023.162629

Ge, M., Wang, X., Du, M., et al. (2019). Adsorption Analyses of Phenol from Aqueous Solutions Using Magadiite Modified with Organo-Functional Groups: Kinetic and Equilibrium Studies. *Materials, 12*, 96. https://doi.org/10.3390/ma12010096

Giles, C., Smith, D., & Huitson, A. (1974). A general treatment and classification of the solute adsorption isotherm. I. Theoretical. *Journal of Colloid and Interface Science, 47*, 755–765. https://doi.org/10.1016/0021-9797(74)90252-5

Gkika, D., Mitropoulos, A., & Kyzas, G. (2022). Why reuse spent adsorbents? The latest challenges and limitations. *Science of the Total Environment, 822*, Article 153612. https://doi.org/10.1016/j.scitotenv.2022.153612

Gundogdu, A., Duran, C., Senturk, B., et al. (2012). Adsorption of phenol from aqueous solution on a low-cost activated carbon produced from Tea Industry Waste: Equilibrium, kinetic, and thermodynamic study. *Journal of Chemical and Engineering Data, 57*, 2733–2743. https://doi.org/10.1021/je300597u

Hamadneh, I., Abu-Zurayk, R., & Al-Dujaili, A. (2020). Removal of phenolic compounds from aqueous solution using MgCl2-impregnated activated carbons derived from olive husk: The effect of chemical structures. *Water Science and TechnoloGy, 81*, 2351–2367. https://doi.org/10.2166/wst.2020.297

Ho, S. (2022). Low-cost adsorbents for the removal of phenol/phenolics, pesticides, and dyes from wastewater systems: A review. *Water, 14*, Article 3203. https://doi.org/10.3390/w14203203

Honarmandrad, Z., Javid, N., & Malakootian, M. (2021). Removal efficiency of phenol by ozonation process with calcium peroxide from aqueous solutions. *Applied Water Science, 11*, Article 14. https://doi.org/10.1007/s13201-020-01344-7

Hossain, M. F., Akther, N., Lu, J., et al. (2025). Highly effective and reusable cellulose-based amphoteric adsorbent for dye removal from single and binary system. *International Journal of Environmental Science and Technology, 22*, 10083–10102. https://doi.org/10.1007/s13762-024-06265-5

Huaxu, L., Fuqiang, W., Dong, Z., et al. (2020). Experimental investigation of cost-effective ZnO nanofluid based spectral splitting CPV/T system. *Energy, 194*, Article Article 116913. https://doi.org/10.1016/j.energy.2020.116913

Ighalo, J., Omoarukhe, F., Ojukwu, V., et al. (2022). Cost of adsorbent preparation and usage in wastewater treatment: A review. *Cleaner Chemical Engineering, 3*, Article Article 100042. https://doi.org/10.1016/j.clce.2022.100042

Ihsanullah, I., Khan, M., Zubair, M., Bilal, M., & Sajid, M. (2022). Removal of pharmaceuticals from water using sewage sludge-derived biochar: A review. *Chemosphere, 289*, Article Article 133196. https://doi.org/10.1016/j.chemosphere.2021.133196

Khalid, K., Joly, G., Renaud, A., et al. (2004). Removal of phenol from water by adsorption using zeolites. *Industrial & Engineering Chemistry Research, 43*, 5275–5280. https://doi.org/10.1021/ie0400447

Khoj, M. (2024). Fabrication of silica/calcium alginate nanocomposite based on rice husk ash for efficient adsorption of phenol from water. *RSC Advances, 14*, 24322. https://doi.org/10.1039/d4ra04070h

Kumar, P., Korving, L., van Loosdrecht, M., et al. (2019). Adsorption as a technology to achieve ultra-low concentrations of phosphate: Research gaps and economic analysis. *Water Research X, 4*, Article Article 100029. https://doi.org/10.1016/j.wroa.2019.100029

Kusmierek, K., & Swiatkowski, A. (2023). Adsorption of phenols on carbonaceous materials of various origins but of similar specific surface areas. *Separations, 10*, Article 422. https://doi.org/10.3390/separations10080422

Kyziol-Komosinska, J., Dzieniszewska, A., & Pasieczna-Patkowska, S. (2024). Compost as green adsorbent for the Azo dyes: Structural characterization and dye removal mechanism. *Korean Journal of Chemical Engineering, 41*, 3227–3243. https://doi.org/10.1007/s11814-024-00254-7I

Liu, B., Yang, F., Zou, Y., et al. (2014). Adsorption of phenol and p-nitrophenol from aqueous solutions on metal-organic frameworks: Effect of hydrogen bonding. *Journal of Chemical & Engineering Data, 59*, 1476–1482. https://doi.org/10.1021/je4010239

Liu, Y., Li, W., Sun, X., Li, S., Wang, C., & Zhang, R. (2023). Adsorption of lead ions by green waste compost and its mechanism. *Journal of Soils and Sediments, 23*, 299–311.

Mamman, S., Yaacob, S., Raoov, M., et al. (2023). Exploring the performance of magnetic methacrylic acid-functionalized β-cyclodextrin adsorbent toward selected phenolic compounds. *Journal of Analytical Science and Technology, 14*, Article 3. https://doi.org/10.1186/s40543-023-00367-4

Mussa, S., Farhan, M., Ahmad, S., et al. (2025). Exploring the utility of different bulking agents for speeding up the composting process of household kitchen waste. *Scientific Reports, 15*, Article 2488. https://doi.org/10.1038/s41598-025-85433-0

Nadavala, S., Che Man, H., & Woo, H. (2014). Biosorption of phenolic compounds from aqueous solutions using pine (*Pinus densiflora* Sieb) bark powder. *BioResources, 9*, 5155–5174. https://doi.org/10.15376/biores.9.3.5155-5174

NIH, National Library for Medicine. (2025). https://pubchem.ncbi.nlm.nih.gov. Accessed 1 Feb 2026.

Paradelo, R., Al-Zawahreh, K., & Barral, M. (2020). Utilization of composts for adsorption of methylene blue from aqueous solutions: Kinetics and equilibrium studies. *Materials, 13*(9), Article 2179. https://doi.org/10.3390/ma13092179

Paredes, C., Roig, A., Bernal, M., et al. (2000). Evolution of organic matter and nitrogen during co-composting of olive mill wastewater with solid organic wastes. *Biology and Fertility of Soils, 32*, 222–227. https://doi.org/10.1007/s003740000239

Ramisio, P., Bento, F., Geraldo, D., Andrade, O., & Bettencourt, A. (2023). Evaluation of municipal waste compost in relation to the environmental retention of heavy metals. *Sustainability, 15*, Article 16395.

Rynk, R., Franciosi, F., Weindorf, D., et al. (2021). *The Composting Handbook* (1st ed.). Elsevier.

Sajid, M., Ihsanullah, I., Khan, M., & Baig, N. (2023). Nanomaterials-based adsorbents for remediation of microplastics and nanoplastics in aqueous media: A review. *Separation and Purification Technology, 305*, Article 122453. https://doi.org/10.1016/j.seppur.2022.122453

Samrane, K., & Bouhaouss, A. (2022). Experimental tests of cadmium and trace metals adsorption on natural clays and activated carbon from wet phosphoric acid. *Inorganic Chemistry Communications, 144*, Article 109866. https://doi.org/10.1016/j.inoche.2022.109866

Sarker, N., & Fakhruddin, A. (2017). Removal of phenol from aqueous solution using rice straw as adsorbent. *Applied Water Science, 7*, 1459–1465. https://doi.org/10.1007/s13201-015-0324-9

Sharanyakanth, P., & Radhakrishnan, M. (2020). Synthesis of metal-organic frameworks (MOFs) and its application in food packaging: A critical review. *Trends in Food Science & Technology, 104*, 102–116. https://doi.org/10.1016/j.tifs.2020.08.004

Smidt, E., & Meissl, K. (2006). The applicability of Fourier transform infrared (FT-IR) spectroscopy in waste management. *Waste Management, 27*, 268–276. https://doi.org/10.1016/j.wasman.2006.01.016

US EPA. (2014). *Toxic and priority pollutants under the clean water act*. US EPA. https://19january2017snapshot.epa.gov/eg/toxic-and-priority-pollutants-under-clean-water-act_.html. Accessed 1 Feb 2026.

Vasiljević, T., Spasojević, J., Baćić, M., et al. (2006). Adsorption of phenol and 2,4-dinitrophenol on activated carbon cloth: The influence of sorbent surface acidity and pH. *Separation Science and Technology, 41*, 1061–1075. https://doi.org/10.1080/01496390600588853

Vergnoux, A., Guiliano, M., Le Dreau, Y., et al. (2009). Monitoring of the evolution of an industrial compost and prediction of some compost properties by NIR spectroscopy. *Science of the Total Environment, 407*, 2390–2403. https://doi.org/10.1016/j.scitotenv.2008.12.033

Wang, P., Changa, C., Watson, M., et al. (2004). Maturity indices for composted dairy and pig manures. *Soil Biology & Biochemistry, 36*, 767–776. https://doi.org/10.1016/j.soilbio.2003.12.012

Yang, S., Chen, D., Li, N., et al. (2016). Surface-nano-engineered bacteria for efficient local enrichment and biodegradation of aqueous organic wastes: Using phenol as a model compound. *Advanced Materials, 28*, 2916–2922. https://doi.org/10.1002/adma.201505493

Yun, M., Li, C., Duan, Y., Chi, X., Zhu, X., Ma, J., Shen, B., Feng, S., & Zhang, Z. (2025). Classification of bulking agents and their regulations on composting: A review. *Journal of Environmental Chemical Engineering, 13*, Article 117318. https://doi.org/10.1016/j.jece.2025.117318